

# Characterization of a Chemical Affinity Probe Targeting Akt Kinases

Fiona Pachl,<sup>†</sup> Patrik Plattner,<sup>‡</sup> Benjamin Ruprecht,<sup>†</sup> Guillaume Médard,<sup>†</sup> Norbert Sewald,<sup>‡</sup> and Bernhard Kuster<sup>\*,†,§</sup>

<sup>†</sup>Chair for Proteomics and Bioanalytics, Center of Life and Food Sciences Weihenstephan, Technische Universität München, Emil-Erlenmeyer-Forum 5, 85354 Freising, Germany

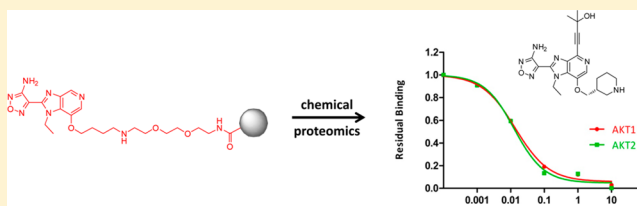
<sup>‡</sup>Organic and Bioorganic Chemistry, Department of Chemistry, Bielefeld University, Bielefeld, Germany

<sup>§</sup>Center for Integrated Protein Science Munich, Emil-Erlenmeyer-Forum 5, 85354 Freising, Germany

## S Supporting Information

**ABSTRACT:** Protein kinases are key regulators of cellular processes, and aberrant function is often associated with human disease. Consequently, kinases represent an important class of therapeutic targets and about 20 kinase inhibitors (KIs) are in clinical use today. Detailed knowledge about the selectivity of KIs is important for the correct interpretation of their pharmacological and systems biological effects. Chemical proteomic approaches for systematic kinase inhibitor selectivity profiling have emerged as important molecular tools in this regard, but the coverage of the human kinome is still incomplete. Here, we describe a new affinity probe targeting Akt and many other members of the AGC kinase family that considerably extends the scope of KI profiling by chemical proteomics. In combination with the previously published kinobeads, the synthesized probe was applied to selectivity profiling of the Akt inhibitors GSK690693 and GSK2141795 in human cancer cells. The results confirmed the inhibition of all Akt isoforms and of a number of known as well as CDC42BPB as a novel putative target for GSK690693. This work also established, for the first time, the kinase selectivity profile of the clinical phase I drug GSK2141795 and identified PRKG1 as a low nanomolar kinase target as well as the ATP-dependent 5'-3' DNA helicase ERCC2 as a potential new non-kinase off-target.

**KEYWORDS:** chemical proteomics, kinobeads, Akt, mass spectrometry



## INTRODUCTION

Protein kinases play a pivotal role in signal transduction and therefore are attractive drug targets in diseases such as cancer and inflammation.<sup>1–5</sup> To date, about 20 small-molecule drugs are approved for clinical use (all in oncology) and several hundred further compounds are under investigation in clinical trials.<sup>6</sup> Most of these agents exert their inhibitory effects via binding to the structurally highly conserved ATP-binding pocket within the kinase domain. As a result, kinase inhibitors (KIs) are likely to target multiple protein kinases or ATP-hydrolyzing/binding enzymes, making the discovery of truly selective inhibitors a formidable challenge. In a physiological context, off-targets may lead to undesired side effects but may also increase the therapeutic potential of a drug. Hence, determining an inhibitor's full protein selectivity profile is important for the correct interpretation of its biological effects on a cellular and organismal level. Traditional methods to assess the selectivity of kinase inhibitors are based on in vitro kinase activity assays using large panels of recombinant kinases.<sup>7–9</sup> Despite being powerful and widely used, these panels have shortcomings: notably, they mostly utilize an exogenously expressed catalytic kinase domain, thus ignoring regulatory sequence elements present in the full-length protein, activity-regulating posttranslational modifications, and the influence of further proteins and cofactors present in cells.<sup>10,11</sup>

To complement such in vitro assays, affinity-based chemical proteomic methods have been developed to allow for a more unbiased analysis of a drug's potential to interact with kinases or other cellular proteins. One such successful approach makes use of immobilized low-selectivity kinase inhibitors for the specific enrichment of a large subset of the native kinome and other nucleotide binding proteins directly from cell or tissue extracts of biological significance (exemplified by the kinobead technology).<sup>12–16</sup> Kinobeads enable differential profiling of kinase expression in cells and tissues and, when configured as a competition binding assay in conjunction with quantitative mass spectrometry, allow for determination of the selectivity of a small-molecule kinase inhibitor against hundreds of proteins in a single experiment.<sup>17–20</sup> Despite conceptual advantages, chemical proteomic methods also have shortcomings, notably incomplete coverage of the kinome. For example, the published kinobead method,<sup>12</sup> which uses a mixture of seven immobilized kinase inhibitors, does not effectively address Akt kinases due to the lack of suitable affinity probes. The serine/threonine kinase Akt, also known as protein kinase B, belongs to the AGC subfamily of protein kinases and is a key mediator of cell growth, proliferation, and apoptosis.<sup>21,22</sup> Aberrant activation of

Received: May 15, 2013

Published: June 25, 2013

the Akt pathway has been identified in a wide variety of human cancers including tumors of the breast, prostate, ovaries, and skin.<sup>23–26</sup> Therefore, inhibiting Akt activity is viewed as an attractive therapeutic approach, and several small-molecule inhibitors targeting this enzyme have been reported and are being tested in the clinic.<sup>27–29</sup> Given the above shortcomings, we sought to develop a chemical affinity probe targeting Akt and structurally related kinases in order to expand the kinome coverage of kinobeads. This was achieved by retroengineering the potent and reasonably selective Akt inhibitor GSK690693<sup>27</sup> into a broad kinase binder. In combination with the previous version of kinobeads, the new Akt probe enabled us to determine the selectivity profile of the ATP-competitive Akt inhibitors GSK690693 and GSK2141795<sup>30</sup> and to identify a number of off-targets that may be responsible for desired and undesired biological effects.

## MATERIALS AND METHODS

### Chemical Synthesis

Synthetic schemes, detailed procedures, and characterization of synthesized compounds can be found in the Supporting Information.

### Sample Preparation

Postdelivery human placenta tissue (obtained from Freising hospital following informed consent) was thoroughly washed with cold phosphate-buffered saline (PBS) and homogenized in lysis buffer (50 mM Tris-HCl, pH 7.5, 5% glycerol, 1.5 mM MgCl<sub>2</sub>, 150 mM NaCl, 0.8% NP-40, 1 mM dithiothreitol, and 25 mM NaF with freshly added protease inhibitors and phosphatase inhibitors) by use of a tissue grinder. Lysates were incubated for 30 min at 4 °C, and protein extracts were clarified by ultracentrifugation for 1 h at 145000g at 4 °C. Protein concentration was determined by the Bradford method.

K562 and COLO205 cells were cultured in Roswell Park Memorial Institute 1640 (RPMI 1640) medium, SKNB2 cells were cultured in Dulbecco's modified Eagle's medium (DMEM), and OVCAR8 cells were cultured in Iscove's modified Dulbecco's medium (IMDM), all supplemented with 10% fetal bovine serum (FBS). Cells were cultured in humidified air supplemented with 5% CO<sub>2</sub> at 37 °C. Cells were washed with cold PBS and harvested by lysis in 50 mM Tris-HCl, pH 7.5, 5% glycerol, 1.5 mM MgCl<sub>2</sub>, 150 mM NaCl, 0.8% NP-40, 1 mM dithiothreitol, and 25 mM NaF with freshly added protease inhibitors and phosphatase inhibitors (5× phosphatase inhibitor cocktail 1, Sigma–Aldrich, Munich, Germany; 5× phosphatase inhibitor cocktail 2, Sigma–Aldrich, Munich, Germany; 1 mM Na<sub>3</sub>VO<sub>4</sub>; and 20 nM calyculin A, LC Laboratories, Woburn, MA). Protein extracts were clarified by ultracentrifugation for 1 h at 145000g at 4 °C, and protein concentration was determined by the Bradford method.

### Compound Coupling

Compounds were immobilized on Sepharose beads through covalent linkage via primary amino (compound) and carboxyl groups as described previously.<sup>12</sup> One milliliter of *N*-hydroxysuccinimide (NHS) activated Sepharose (GE Healthcare, Freiburg, Germany) and the compound (2 μmol/mL) were equilibrated in dimethyl sulfoxide (DMSO). Triethylamine (15 μL) was added to start the coupling reaction, and the mixture was incubated on an end-over-end shaker for 16–20 h in the dark. Free NHS groups on the beads were blocked by adding 50 μL of aminoethanol and the mixture was

incubated on an end-over-end shaker for 16–20 h in the dark. Coupled beads were washed and stored in 2-propanol at 4 °C in the dark. The coupling reaction was monitored by high-performance liquid chromatography (HPLC).

### Compound Deprotection

Sepharose beads (2 μmol/mL; 1 mL) functionalized with *o*-nitrobenzenesulfonyl (*o*-Nbs) protected compound were washed and equilibrated in *N,N*-dimethylformamide (DMF). For the deprotection reaction, *N*-methyl-2-pyrrolidone (NMP, 2 mL), 1,8-diazabicyclo[5.4.0]undec-7-ene (DBU, 1.5 mL), and mercaptoethanol (1.5 mL) were added and the mixture was incubated on an end-over-end shaker for 15 min at room temperature. Subsequently, beads were washed and stored in 2-propanol at 4 °C in the dark.

### Affinity Purification

Akt probe and kinobead pulldowns were performed as described previously.<sup>12</sup> Briefly, lysates of a cell mix were diluted with equal volumes of 1× compound pulldown (CP) buffer [50 mM Tris-HCl, pH 7.5, 5% glycerol, 1.5 mM MgCl<sub>2</sub>, 150 mM NaCl, 25 mM NaF, 1 mM dithiothreitol, and freshly added protease inhibitors and phosphatase inhibitors (5× phosphatase inhibitor cocktail 1, Sigma–Aldrich, Munich, Germany; 5× phosphatase inhibitor cocktail 2, Sigma–Aldrich, Munich, Germany; 1 mM sodium orthovanadate; and 20 nM calyculin A, LC Laboratories, Woburn, MA)]. If necessary, lysates were further diluted to a final protein concentration of 5 mg/mL in 1× CP buffer supplemented with 0.4% NP-40.

For selectivity profiling experiments, the lysates (5 mg of total protein each) were preincubated with 0 (DMSO control), 2.5 nM, 25 nM, 250 nM, 2.5 μM or 25 μM free compound (GSK690693 or GSK2141795) on an end-over-end shaker for 45 min at 4 °C. Subsequently, lysates were incubated with beads (coupled Akt probe or kinobeads) for 1 h at 4 °C, for both qualitative and quantitative experiments. The beads were washed with 1× CP buffer and collected by centrifugation. Bound proteins were eluted with 2× NuPAGE LDS sample buffer (Invitrogen, Darmstadt, Germany), and eluates were reduced and alkylated by 50 mM dithiothreitol and 55 mM iodoacetamide.

Samples were then run into a 4–12% NuPAGE gel (Invitrogen, Darmstadt, Germany) for about 0.5 cm to concentrate the sample prior to in-gel tryptic digestion, which was performed according to standard procedures.

### Liquid Chromatography–Tandem Mass Spectrometry Measurements

Nanoflow LC-MS/MS was performed by coupling an Eksigent nanoLC-Ultra 1D+ (Eksigent, Dublin, CA) to a LTQ-Orbitrap XL ETD (Thermo Scientific, Bremen, Germany). Peptides were delivered to a trap column (100 μm × 2 cm, packed in-house with Reprosil-Pur C<sub>18</sub>-AQ 5 μm resin; Dr. Maisch, Ammerbuch, Germany) at a flow rate of 5 μL/min in 100% solvent A (0.1% formic acid in HPLC-grade water). After 10 min of loading and washing, peptides were transferred to an analytical column (75 μm × 40 cm, packed in-house with Reprosil-Pur C<sub>18</sub>-AQ, 3 μm resin; Dr. Maisch, Ammerbuch, Germany) and separated via a 210 min gradient from 7% to 35% solvent B (0.1% formic acid in acetonitrile) at 300 nL/min flow rate. The LTQ Orbitrap XL was operated in data-dependent mode, automatically switching between MS and MS2. Full-scan MS spectra were acquired in the Orbitrap at 60 000 (*m/z* 400) resolution after accumulation to a target

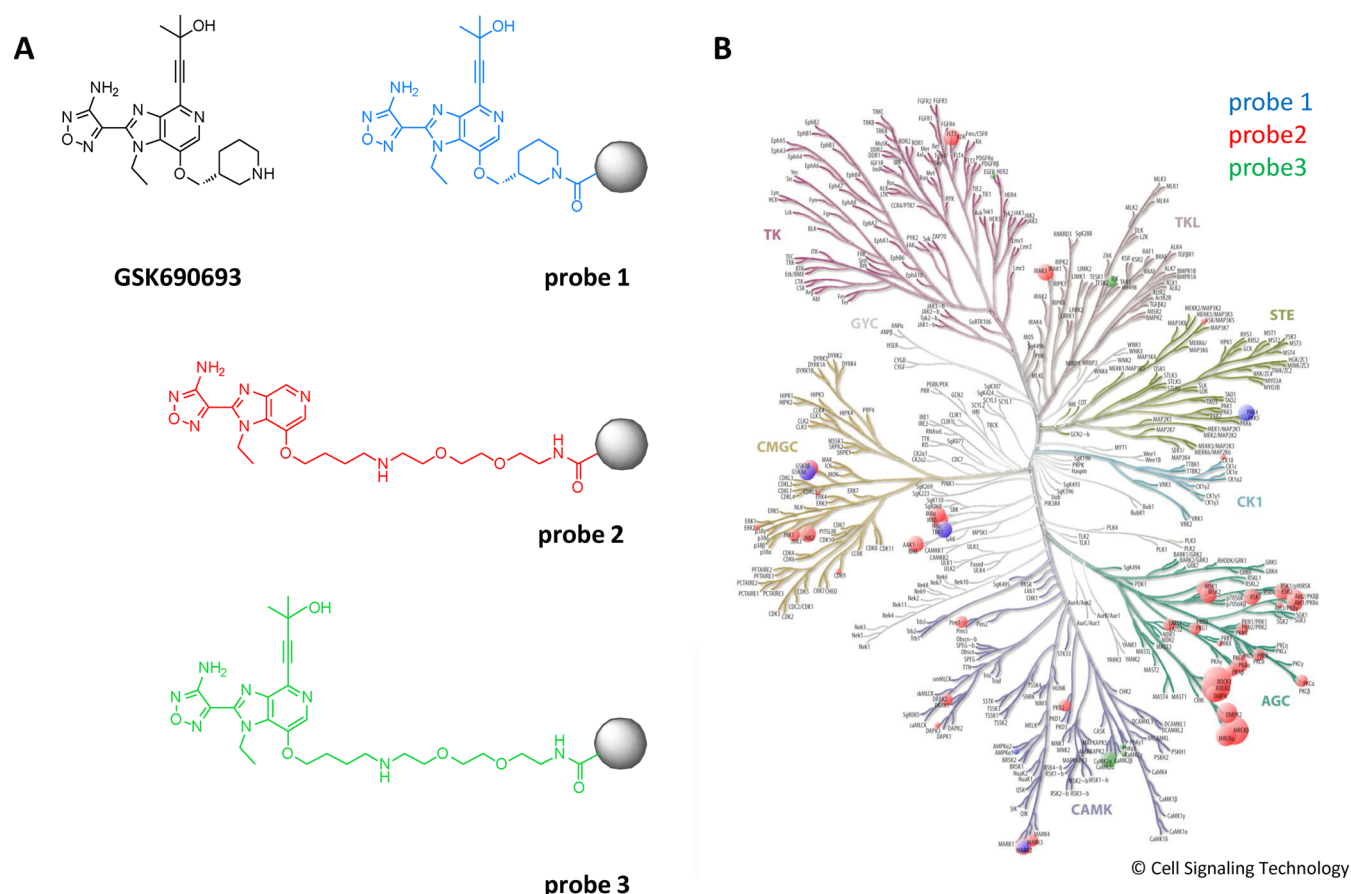


**Figure 1.** Comparison of Akt affinity matrices. (A) Chemical structures of Akt inhibitor GSK690693 and affinity probes 1–3 immobilized on Sepharose beads. (B) Kinome tree representing the different classes of kinases enriched by probe 1 (blue), probe 2 (red), and probe 3 (green). The size of the circle reflects the number of unique spectra assigned to a kinase and serves as a semiquantitative measure for the quantity of an enriched kinase.

value of 1 000 000. Internal calibration was performed by use of the ion signal  $[\text{Si}(\text{CH}_3)_2\text{O}]_6\text{H}^+$  at  $m/z$  445.120 025 present in ambient laboratory air. Tandem mass spectra were generated for up to eight peptide precursors in the linear ion trap for fragment by using collision-induced dissociation at a normalized collision energy of 35% after accumulation to a target value of 5000 for a maximum of 500 ms.

Measurements using the Orbitrap Elite (Thermo Scientific, Bremen, Germany) employed the same LC conditions as described and similar data acquisition parameters. Full-scan MS spectra were acquired in the Orbitrap at 30 000 resolution. Tandem mass spectra were generated for up to 15 peptide precursors for fragment by using higher energy collisional dissociation (HCD) at normalized collision energy of 30% and a resolution of 15 000 with a target value of 100 000 charges after accumulation for a maximum of 100 ms.

#### Peptide and Protein Identification and Quantification

For qualitative analysis, raw MS data files were converted to peak lists by use of Mascot Distiller (version 2.3.0, Matrix Science, London) and searched against the IPI human database (version 3.68; 87 061 sequences) by use of the Mascot search engine (version 2.3.0, Matrix Science, London) and the following parameters: precursor tolerance 10 ppm, fragment tolerance 0.6 Da, full tryptic specificity with up to two missed cleavage sites, and misassignment of the monoisotopic peak to the first  $^{13}\text{C}$  peak, fixed modification of carbamidomethylation of cysteine residues, and variable modification of methionine

oxidation. The database search results were imported into Scaffold (version 3.6.2, Proteome Software, Portland, OR) for further evaluation.

Quantitative analysis with intensity-based label-free quantification was performed by the Progenesis software (version 3.1, Nonlinear Dynamics, Newcastle, U.K.). Briefly, after one sample was selected as a reference, the retention times of all eluting precursor  $m/z$  values in all other samples within the experiment were aligned, creating a large list of “features” representing the same peptide in each sample. Features with 2–5 charges were included for further analysis. Features with two or less isotopes were excluded. After alignment and feature filtering, replicate samples were grouped together, and raw abundances of all features were normalized to determine a global scaling factor for correcting experimental variation such as differences in the quantity of protein loaded into the instrument. Briefly, for each sample, one unique factor is calculated and used to correct all features in the sample for experimental variation according to Hauck et al.<sup>31</sup> MS/MS spectra were transformed into peak lists and exported to generate Mascot generic files. The Mascot generic files were searched against the protein sequence database IPI human (version 3.68; 87 061 sequences) by use of Mascot (version 2.3.0, Matrix Science, London). Search parameters were as follows: precursor tolerance 10 ppm, fragment tolerance 0.02 Da, full tryptic specificity with up to two missed cleavage sites, misassignment of the monoisotopic peak to the first  $^{13}\text{C}$  peak, fixed modification of carbamidome-



Table 1. List of Kinases Identified in Pulldowns by Use of Probes 1, 2, and 3 from Human Placenta Lysate<sup>a</sup>

gene name	IPI-ID	no. of unique peptides			gene name	IPI-ID	no. of unique peptides		
		probe 1	probe 2	probe 3			probe 1	probe 2	probe 3
AAK1	IPI00916402		34		MARK2	IPI00555838	7	25	
Akt1	IPI00012866		12		MARK3	IPI00220506		8	
Akt2	IPI00012870		14		MTOR	IPI00031410			2
Akt3	IPI00031747		4		PAK4	IPI00014068	11		
CAMK2D	IPI00172636		21	21	PHKG2	IPI00012891			2
CAMK2G_Iso6	IPI00908444		4	2	PI4KA	IPI00070943			69
CAMK2G_Iso7	IPI00915309		39	25	PIM1	IPI00005014		7	
CDC42BPA	IPI00640957		57		PKN2	IPI00002804		10	
CDC42BPB	IPI00477763		205		PRKAA1	IPI00410287	2	2	3
CDC42BPG	IPI00454910		68		PRKAB2	IPI00013905		6	
CDK9	IPI00301923		3		PRKACA	IPI00396630		43	
CDKL5	IPI00746301		3		PRKACB	IPI00395654		10	
CHUK	IPI00005104		20		PRKCA	IPI00385449		7	
CSNK1D	IPI00011102		4		PRKCD	IPI00329236		7	
DAPK3	IPI00015213		3		PRKCZ	IPI00013749		3	
DMPK	IPI00215958		15		PRKD2	IPI00009334		9	
EGFR	IPI00018274			2	PRKDC	IPI00296337		86	79
FLT1	IPI00018335		14		PRKG1A	IPI00427586		91	6
GSK3A	IPI00292228	22	23		PRKG1B	IPI00436355		9	
GSK3B	IPI00216190	38	37		PRKX	IPI00020904		2	
IKBKB	IPI00024709		39		ROCK1	IPI00022542		137	
ILK	IPI00013219			6	ROCK2	IPI00307155		124	
IRAK3	IPI00026984		11		RPS6KA1	IPI00017305		12	
LATS1	IPI00005858		7		RPS6KA3	IPI00020898		35	
MAP3K5	IPI00412433		4		RPS6KA4	IPI00022536		25	
MAPK1	IPI00003479		5		RPS6KA5	IPI00335101		30	
MAPK8	IPI00220305		10		STK17B	IPI00014934		6	
MAPK9	IPI00024673		13		TBK1	IPI00293613	19	20	

<sup>a</sup>For a complete list of identified proteins, see Table S1 in Supporting Information.

thylation of cysteine residues, and variable modification of N-terminal protein acetylation and methionine oxidation. Search results for spectrum to peptide matches were exported in .xml format and then imported into Progenesis software to enable the combination of peptide quantification and identification. Peptides with mascot ion scores  $\leq 32$  ( $p = 0.05$  identity threshold) were filtered out, and only unique peptides for corresponding proteins were used for identification and quantification. In dose–response measurements, protein quantification was performed by summing the feature intensities of all unique peptides of a protein.

## RESULTS AND DISCUSSION

### Design and Synthesis of Affinity Probes Targeting Akt and AGC Family Kinases

The potent ATP-competitive Akt inhibitor GSK690693 (Figure 1A) was chosen as starting point for the design of chemical affinity probes, as this compound inhibits all three isoforms of Akt (1, 2, and 3) at low nanomolar concentrations and further shows potent activity against a number of AGC family members as well as other protein kinases.<sup>27</sup> For affinity probes intended for KI selectivity profiling, low kinase selectivity (but potent binding) is desirable in order to enable the measurement of many kinases simultaneously. We therefore explored the merits of three linkable compounds (Figure 1A): probe 1 corresponds to the parental compound, which can be immobilized via its secondary amine. Considerations leading to the design and synthesis of probes 2 and 3 (see Supporting Information for

details) were based on the cocrystal structure of GSK690693 and the kinase domain of Akt2 (PDB code 3DOE; Figure S1, Supporting Information) as well as the described structure–activity relationship (SAR) of GSK690693.<sup>27</sup> The inhibitor occupies the ATP binding pocket with the 1,2,5-oxadiazole moiety located in the hinge region. Several inter- and intramolecular hydrogen bonds of the 1,2,5-oxadiazole and the imidazopyridine ring, together with hydrophobic interactions with the glycine-rich loop, provide strong interactions between kinase and inhibitor. Furthermore, the alkynol group at position C4 of the imidazopyridine core is located in the back cleft pocket and improves potency for Akt and, importantly, selectivity against other kinases of the AGC family.<sup>27</sup> The piperidiny side chain is exposed to the solvent and also provides hydrogen bonding to the carboxylic acid side chain of Glu 236 in the substrate binding area of Akt. This feature makes this side of the molecule attractive for modification with a linker, provided that the basicity of the amino group can be kept intact. Structural and SAR information together would predict that probe 3 should be more selective for Akt than probe 2.

### Protein Binding Profiles of Akt Probes

The protein binding profiles of the three immobilized compounds (probes 1, 2, and 3) were assessed in pulldown experiments on lysates of human placenta, followed by mass spectrometry for protein identification. A triplicate analysis resulted in the identification of 204 proteins (six kinases) for probe 1, 347 proteins (50 kinases) for probe 2, and 458



**Figure 2.** Comparison of the enrichment profiles of kinobeads without (KBα) and with (KBβ) addition of probe 2. The heat map shows the identified kinases, with the number of unique spectra as a semiquantitative measure of the quantity of an enriched kinase. The darker the color, the more abundant the enriched kinase. Addition of probe 2 adds significantly to the kinome coverage of kinobeads.

proteins (11 kinases) for probe 3 (see Table 1 for kinases and Table S1, Supporting Information, for all proteins). This clearly identified probe 2 as the most effective kinase binder, and in fact the only one capable of capturing all three isoforms of Akt. Visualization of the identified kinases on the phylogenetic kinome tree (Figure 1B) revealed that probe 2 captures a considerable number of further AGC kinases as well as members of the CMGC and CAMK kinase families. The broad kinase binding profile can be rationalized (i) by the high structural conservation of the kinase domain and ATP binding pocket within the AGC family and (ii) by the removal of the alkynol moiety, which was previously shown to improve selectivity, for example, against ROCK and RSK.<sup>27</sup> Probes 1 and 3 were ineffective in capturing Akt and also captured only a few other kinases. This may not be surprising for probe 1, as the basicity of the secondary amine of the piperidinyl side chain present in GSK690693 and important for Akt binding is not preserved in the immobilized configuration. The fairly low degree of kinase binding may be rationalized by the rather short and bulky group attaching the compounds to the beads, which may prevent the molecule from reaching deep enough into the ATP binding pocket. This argument does not apply for probe 3, as its linker is the same as that of probe 2. Instead, it is possible that the functional alkynol group cannot efficiently penetrate the very narrow opening into the back pocket of the ATP binding site of kinases, so that even small conformational

changes in the compound and/or the native, full-length protein structure might considerably impair proper binding. It is noteworthy, though, that probe 3 appears to be an effective binder for the phosphatidylinositol kinase PI4KA, a lipid kinase that has recently been implicated in hepatitis C replication in human cells.<sup>32</sup>

Apart from kinases, the three probes bind to multiple other proteins. This is not unusual: proteins may bind unspecifically to the beads, but also the immobilized KIs are ATP mimetics that have the potential to bind nucleotide binding proteins, of which there are many hundreds in mammalian cells. Gene ontology (GO) analysis of the identified proteins (Figure S2, Supporting Information) reveals that all probes do bind a considerable number of these proteins as well as further RNA/DNA binding proteins. When the number of unique tandem mass spectra of identified proteins is used as a semiquantitative measure for protein abundance, it can be noted that about two-thirds of the total proteins binding to probe 2 can be rationalized by one of the aforementioned GO categories. In contrast, less than one-third of these proteins explain the binding profiles of probes 1 and 3.

Having established that probe 2 is an effective affinity tool for capturing protein kinases, notably of the AGC branch, we next investigated whether the probe would extend the kinome coverage of kinobeads as published by Bantscheff et al.<sup>12</sup> For this purpose, we performed pulldown experiments (in

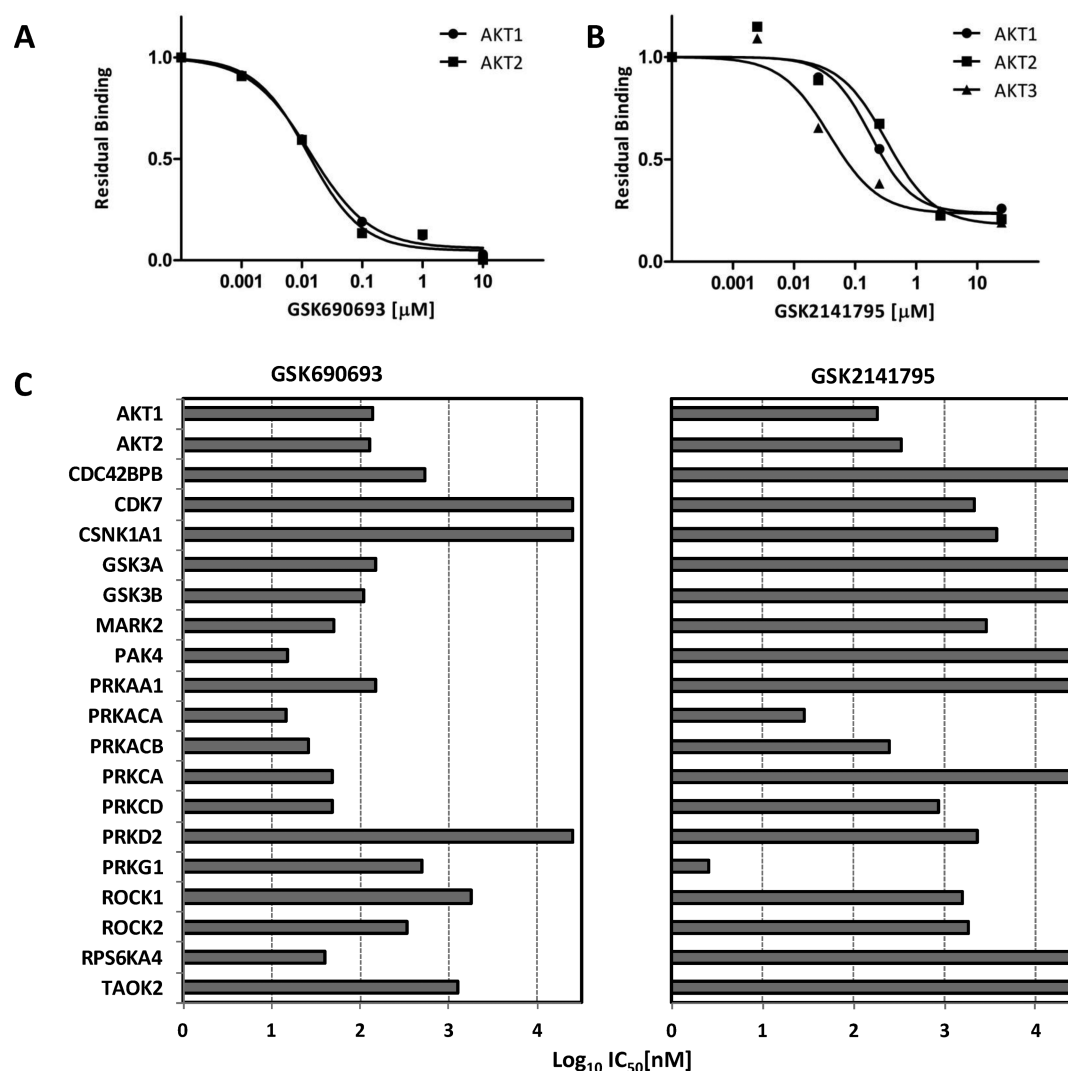


**Figure 3.** Target selectivity profiles of the clinical Akt inhibitors GSK690693 and GSK2141795. (A, B) Competition binding curves for identified isoforms of the primary target Akt. (C) Comparison of proteomic target profiles of GSK690693 and GSK2141795. It is evident that the selectivity range of GSK2141795 is much narrower than that of GSK690693. Only targets identified in both data sets are shown.

triplicate) from lysates of human placenta using either kinobeads as published (seven immobilized compounds, KB $\alpha$ ) or kinobeads supplemented with probe 2 (KB $\beta$ ). In pull-downs with KB $\alpha$ , 130 kinases (total of 860 proteins; Figure 2; Figures S3 and S4 and Table S3, Supporting Information) were identified and KB $\beta$  pull-down experiments led to the identification of 139 kinases out of a total of 815 proteins. As expected, more than 80% of the protein kinases were identified in both experiments. Twenty-three kinases (15 from the AGC family) were exclusively found in the KB $\beta$  experiment (Figure S3B,C, Supporting Information), and members of the AGC family were present in significantly higher amounts on KB $\beta$  compared to KB $\alpha$  (Figure S4 and Table S2, Supporting Information). The 14 kinases exclusively identified on KB $\alpha$  originate from many different areas of the kinome tree and these hits were mostly identified with few spectra (Table S2, Supporting Information), thus representing kinases with either low affinity to the kinobeads or kinases of very low abundance in the sample. Taken together, probe 2 both qualitatively and quantitatively adds to the published version of kinobeads, which is why this chemical affinity tool was used for all subsequent experiments.

### Kinase Inhibitor Selectivity Profile

To demonstrate the utility of the new kinobeads KB $\beta$ , we subjected the Akt inhibitors GSK690693<sup>33–35</sup> (phase I, terminated) and GSK2141795<sup>30</sup> (active phase I trials in patients with solid tumors or lymphomas) to kinase selectivity profiling in mixed lysates of four cancer cells (see Materials and Methods section). Briefly, KB $\beta$  pull-downs were performed after preincubation of separate lysates with increasing concentrations of the respective drug. Protein targets that bind the drug in the lysate show a dose-dependent reduction in binding to the kinobeads, while proteins unaffected by the drug show no reduction in binding. Proteins were eluted from kinobeads, digested with trypsin into peptides, and analyzed by liquid chromatography–tandem mass spectrometry (LC-MS/MS).<sup>36</sup> Following protein identification by database searching, proteins were quantified by use of their LC-MS/MS intensities, and dose–response curves were generated from the resulting data (Figure S5, Supporting Information). The results of these experiments show clear similarities as well as differences in the selectivity profiles of the two compounds. Both expectedly show inhibition of Akt1 and 2 (Figure 3A,B and Table 2; Akt3 was detected only in assays with GSK2141795), and  $IC_{50}$  values

**Table 2. Comparative List of Putative Targets of GSK690693 and GSK2141795 with IC<sub>50</sub> Values<sup>a</sup>**

kinase	IC <sub>50</sub> (nM)	
	GSK690693	GSK2141795
Akt1	138	180
Akt2	128	328
CDC42BPB	550	>10 000
CDK7	>10 000	2100
CSNK1A1	>10 000	3690
GSK3A	147	>10 000
GSK3B	111	>10 000
MARK2	50	2900
PAK4	15	>10 000
PRKAA1	148	>10 000
PRKACA	14	29
PRKACB	26	249
PRKCA	49	>10 000
PRKCD	48	849
PRKD2	>10 000	2260
PRKG1	497	3
ROCK1	1808	1570
ROCK2	340	1850
RPS6KA4	40	>10 000
TAOK2	1285	>10 000

<sup>a</sup>As determined by the kinobead competition binding assay.

of 138 nM (Akt1) and 128 nM (Akt2) were determined for GSK690693. GSK2141795 inhibited kinobead binding with IC<sub>50</sub> values of 180 nM for Akt1, 328 nM for Akt2, and 38 nM for Akt3 (Table 2). We note here that IC<sub>50</sub> values for target affinities determined in such competition binding assays are often affected by the partial depletion of individual target proteins from the lysate. This can be compensated for by calculating a target-specific  $K_D$  value using a correction factor derived from the Cheng–Prusoff equation.<sup>16,37</sup> This results in  $K_D$  values of 16 nM for Akt1, 49 nM for Akt2, and 5 nM for Akt3 (for GSK2141795), which are in line with literature data from biochemical assays that report potencies of 2 nM for Akt1, 2–13 nM for Akt2, and 3–9 nM Akt3 for GSK690693.<sup>7,27,34</sup> We further note that compound potencies determined by kinobead assays are often weaker than those obtained from biochemical kinase assays. We attribute this to fundamental differences in assay conditions: in vitro kinase assays generally measure isolated recombinant kinase domains, while the kinobead assay measures full-length native kinases expressed in cell lines or tissues. In addition, the respective lysates contain other cellular proteins and cofactors not present in recombinant assays that might regulate kinase activity or otherwise interfere with or bind to the free compound (e.g., acting as a compound sink).

Apart from Akt, the profile of GSK690693 contains 13 further kinases with submicromolar IC<sub>50</sub> values, in sharp contrast to GSK2141795, for which only four such cases are detected (Figure 3C and Table 2). The selectivity of GSK690693 toward kinases has been studied before,<sup>7,27,34</sup> documenting low- to midnanomolar binding constants for members of the protein kinase A (13–24 nM) and protein kinase C (2–250 nM) family of proteins, GSK3a (5200 nM) and GSK3b (100–140 nM), ROCK1 (280–890 nM) and ROCK2 (200 nM), MARK2 (720 nM), and RPS6KA4 (51 nM) as well as PAK4 (10–18 nM). These targets are also found in the kinobead assay with binding inhibition values

between 15 and 340 nM. In addition to these previously known targets, our assay revealed binding inhibition of CDC42BPB (also known as MRCKB, IC<sub>50</sub> = 550 nM). Interestingly, the kinase domain of MRCKB resembles that of PAK kinases and it is thus likely that MRCKB constitutes a novel target of GSK690693. Taken together, the selectivity profile of this compound is fairly broad and the particular kinases inhibited should help in understanding the cellular action of the molecule. While anticancer activity of the compound may be rationalized based on several of the inhibited kinases, each playing a role in various types of cancer (e.g., Akt,<sup>21–26</sup> PKC,<sup>38–40</sup> ROCK,<sup>41</sup> PAK,<sup>42</sup> MRCKB<sup>43</sup>), the inhibition of other kinases in the target spectrum may be more problematic. For example, potent inhibition of GSK3 might be a double-edged sword. On the one hand, GSK3 activity has been linked to cancer;<sup>44,45</sup> on the other hand, in concert with Akt and mTOR, GSK3 is an important mediator of the insulin pathway and its inhibition may lead to impaired glucose uptake, induce hyperglycemia, hyperinsulinemia, and glucose intolerance.<sup>46</sup> Similarly, PKA signaling pathways are active in many cell types and mediate a wide spectrum of normal biological functions. If and how pharmacological PKA inhibition might be beneficial for treating cancer or detrimental for normal cells is therefore not necessarily clear.<sup>47,48</sup>

Judged from the kinobead selectivity profile, the target spectrum of GSK2141795 appears to be much narrower than that of GSK690693. Apart from the Akts, only the PKC family members PRKACA and PRKACB as well as the cGMP-dependent protein kinase PRKG1 are potently inhibited (Table 2). The much tighter selectivity profile of GSK2141795 is likely beneficial, as some of the potential biological toxicity issues might be circumvented. Still, while the inhibition of PKCs may contribute to the anticancer effects of this compound, the physiological consequences of the very potent inhibition (IC<sub>50</sub> = 2.5 nM,  $K_d$  = 0.05 nM) of PRKG1 cannot be clearly anticipated at present. This kinase is a key mediator of a plethora of normal cellular and organ functions such as modulation of cellular calcium, platelet activation, smooth muscle contraction, axonal guidance, and learning, to name a few,<sup>49–52</sup> which on their own or in combination might indicate toxic side effects. However, results of ongoing phase I clinical trials have not been reported thus far, referring any such considerations into the realm of speculation at the present time. Given that kinobeads not only bind kinases and other nucleotide binding proteins but also capture binding proteins from cell lysates under denaturing conditions, one frequently observes non-kinase targets and copurification of interacting proteins in competition binding experiments (Figure S6, Supporting Information). For example, spectrin  $\alpha$ 1 (SPTAN1) shows a dose-dependent reduction in binding to kinobeads. This protein contains an SH3 domain, suggesting that it might copurify with a phosphorylated kinase that itself is inhibited by GSK2141795. The ATP-dependent 5′-3′ DNA helicase ERCC2 also shows a dose-dependent reduction of kinobead binding in response to drug treatment. Given the ATP-hydrolyzing activity of this enzyme, which is involved in nucleotide excision repair following DNA damage, it is tempting to speculate that it might be a non-kinase off-target of GSK2141795. How this might impact the phenotype of cells treated with the compound remains to be investigated.



## CONCLUSIONS

In summary, we describe a novel chemical affinity probe for capturing Akt isoforms and about 50 further kinases, primarily from the AGC branch of the kinome phylogenetic tree. This not only increases the range of kinases that can be assayed by the established kinobead technology but also substantially reduces the bias of kinobeads toward the representation of tyrosine and tyrosine-like kinases. Application of the new probes to the selectivity profiling of Akt kinase inhibitors confirmed the broad selectivity of GSK690693 and, for the first time, established the much narrower profile of GSK2141795, generating new hypotheses as to how this clinical Akt inhibitor exerts its cellular effects. Our work shows that retroengineering kinase inhibitors into broad kinase binders works, and it is entirely feasible to apply the same or a similar strategy to other kinase families should reasonable chemical starting points exist. In fact, we are currently in the process of generating probes targeting kinases of the VEGFR and FGFR families, which are not well addressed by existing probes. In light of the current chemoproteomic literature,<sup>37,53,54</sup> it is unlikely that a single true pan-kinase compound probe can be developed, but continuing efforts by ourselves and others in the field<sup>5,55</sup> will likely eventually fill the remaining gaps.

## ASSOCIATED CONTENT

### Supporting Information

Additional text and three schemes, with experimental methods and characterization of compounds, and six figures and three tables as described in the main text. This material is available free of charge via the Internet at <http://pubs.acs.org>.

## AUTHOR INFORMATION

### Corresponding Author

\*E-mail [kuster@tum.de](mailto:kuster@tum.de); tel +49 8161 715696; fax +49 8161 715931.

### Notes

The authors declare no competing financial interest.

## ACKNOWLEDGMENTS

This work was in part funded by the Collaborative Research Center SFB 824. We gratefully acknowledge the Faculty Graduate Center Weihenstephan of the TUM Graduate School at the Technische Universität München, Germany, for financial support (to F.P.). We are also grateful to GlaxoSmithKline for providing a sample of GSK2141795.

## REFERENCES

- (1) Manning, G.; Whyte, D. B.; Martinez, R.; Hunter, T.; Sudarsanam, S. The protein kinase complement of the human genome. *Science* **2002**, 298 (5600), 1912–1934.
- (2) Cohen, P. Protein kinases—the major drug targets of the twenty-first century? *Nat. Rev. Drug Discovery* **2002**, 1 (4), 309–315.
- (3) Fedorov, O.; Muller, S.; Knapp, S. The (un)targeted cancer kinome. *Nat. Chem. Biol.* **2010**, 6 (3), 166–169.
- (4) Page, T. H.; Smolinska, M.; Gillespie, J.; Urbaniak, A. M.; Foxwell, B. M. Tyrosine kinases and inflammatory signalling. *Curr. Mol. Med.* **2009**, 9 (1), 69–85.
- (5) Knapp, S.; Arruda, P.; Blagg, J.; Burley, S.; Drewry, D. H.; Edwards, A.; Fabbro, D.; Gillespie, P.; Gray, N. S.; Kuster, B.; Lackey, K. E.; Mazzaferri, P.; Tomkinson, N. C. O.; Willson, T. M.; Workman, P.; Zuercher, W. J. A public-private partnership to unlock the untargeted kinome. *Nat. Chem. Biol.* **2013**, 9 (1), 3–6.

- (6) Cohen, P.; Alessi, D. R. Kinase drug discovery—what's next in the field? *ACS Chem. Biol.* **2013**, 8 (1), 96–104.

- (7) Davis, M. I.; Hunt, J. P.; Herrgard, S.; Cicceri, P.; Wodicka, L. M.; Pallares, G.; Hocker, M.; Treiber, D. K.; Zarrinkar, P. P. Comprehensive analysis of kinase inhibitor selectivity. *Nat. Biotechnol.* **2011**, 29 (11), 1046–1051.

- (8) Karaman, M. W.; Herrgard, S.; Treiber, D. K.; Gallant, P.; Atteridge, C. E.; Campbell, B. T.; Chan, K. W.; Cicceri, P.; Davis, M. I.; Edeen, P. T.; Faraoni, R.; Floyd, M.; Hunt, J. P.; Lockhart, D. J.; Milanov, Z. V.; Morrison, M. J.; Pallares, G.; Patel, H. K.; Pritchard, S.; Wodicka, L. M.; Zarrinkar, P. P. A quantitative analysis of kinase inhibitor selectivity. *Nat. Biotechnol.* **2008**, 26 (1), 127–132.

- (9) Anastassiadis, T.; Deacon, S. W.; Devarajan, K.; Ma, H.; Peterson, J. R. Comprehensive assay of kinase catalytic activity reveals features of kinase inhibitor selectivity. *Nat. Biotechnol.* **2011**, 29 (11), 1039–1045.

- (10) Nolen, B.; Taylor, S.; Ghosh, G. Regulation of protein kinases; controlling activity through activation segment conformation. *Mol. Cell* **2004**, 15 (5), 661–675.

- (11) Shi, Z.; Resing, K. A.; Ahn, N. G. Networks for the allosteric control of protein kinases. *Curr. Opin. Struct. Biol.* **2006**, 16 (6), 686–692.

- (12) Bantscheff, M.; Eberhard, D.; Abraham, Y.; Bastuck, S.; Boesche, M.; Hobson, S.; Mathieson, T.; Perrin, J.; Raida, M.; Rau, C.; Reader, V.; Sweetman, G.; Bauer, A.; Bouwmeester, T.; Hopf, C.; Kruse, U.; Neubauer, G.; Ramsden, N.; Rick, J.; Kuster, B.; Drewes, G. Quantitative chemical proteomics reveals mechanisms of action of clinical ABL kinase inhibitors. *Nat. Biotechnol.* **2007**, 25 (9), 1035–1044.

- (13) Brehmer, D.; Greff, Z.; Godl, K.; Blencke, S.; Kurtenbach, A.; Weber, M.; Muller, S.; Klebl, B.; Cotten, M.; Keri, G.; Wissing, J.; Daub, H. Cellular targets of gefitinib. *Cancer Res.* **2005**, 65 (2), 379–382.

- (14) Godl, K.; Gruss, O. J.; Eickhoff, J.; Wissing, J.; Blencke, S.; Weber, M.; Degen, H.; Brehmer, D.; Orfi, L.; Horvath, Z.; Keri, G.; Muller, S.; Cotten, M.; Ullrich, A.; Daub, H. Proteomic characterization of the angiogenesis inhibitor SU6668 reveals multiple impacts on cellular kinase signaling. *Cancer Res.* **2005**, 65 (15), 6919–6926.

- (15) Wissing, J.; Jansch, L.; Nimtz, M.; Dieterich, G.; Hornberger, R.; Keri, G.; Wehland, J.; Daub, H. Proteomics analysis of protein kinases by target class-selective prefractionation and tandem mass spectrometry. *Mol. Cell. Proteomics* **2007**, 6 (3), 537–547.

- (16) Sharma, K.; Weber, C.; Bairlein, M.; Greff, Z.; Keri, G.; Cox, J.; Olsen, J. V.; Daub, H. Proteomics strategy for quantitative protein interaction profiling in cell extracts. *Nat. Methods* **2009**, 6 (10), 741–744.

- (17) Wu, Z.; Doondea, J. B.; Gholami, A. M.; Janning, M. C.; Lemeer, S.; Kramer, K.; Eccles, S. A.; Gollin, S. M.; Grenman, R.; Walch, A.; Feller, S. M.; Kuster, B. Quantitative chemical proteomics reveals new potential drug targets in head and neck cancer. *Mol. Cell. Proteomics* **2011**, 10 (12), No. M111 011635.

- (18) Kruse, U.; Bantscheff, M.; Drewes, G.; Hopf, C. Chemical and pathway proteomics: powerful tools for oncology drug discovery and personalized health care. *Mol. Cell. Proteomics* **2008**, 7 (10), 1887–1901.

- (19) Rix, U.; Hantschel, O.; Durnberger, G.; Remsing Rix, L. L.; Planyavsky, M.; Fernbach, N. V.; Kaup, I.; Bennett, K. L.; Valent, P.; Colinge, J.; Kocher, T.; Superti-Furga, G. Chemical proteomic profiles of the BCR-ABL inhibitors imatinib, nilotinib, and dasatinib reveal novel kinase and nonkinase targets. *Blood* **2007**, 110 (12), 4055–4063.

- (20) Daub, H.; Olsen, J. V.; Bairlein, M.; Gnadt, F.; Oppermann, F. S.; Korner, R.; Greff, Z.; Keri, G.; Stemmann, O.; Mann, M. Kinase-selective enrichment enables quantitative phosphoproteomics of the kinome across the cell cycle. *Mol. Cell* **2008**, 31 (3), 438–448.

- (21) Manning, B. D.; Cantley, L. C. Akt/PKB signaling: navigating downstream. *Cell* **2007**, 129 (7), 1261–1274.

- (22) Garcia-Echeverria, C.; Sellers, W. R. Drug discovery approaches targeting the PI3K/Akt pathway in cancer. *Oncogene* **2008**, 27 (41), 5511–5526.



- (23) Altomare, D. A.; Testa, J. R. Perturbations of the Akt signaling pathway in human cancer. *Oncogene* **2005**, *24* (50), 7455–7464.
- (24) Vivanco, I.; Sawyers, C. L. The phosphatidylinositol 3-kinase Akt pathway in human cancer. *Nat. Rev. Cancer* **2002**, *2* (7), 489–501.
- (25) Franke, T. F. PI3K/Akt: getting it right matters. *Oncogene* **2008**, *27* (50), 6473–6488.
- (26) Lu, Y.; Wang, H.; Mills, G. B. Targeting PI3K-Akt pathway for cancer therapy. *Rev Clin Exp Hematol* **2003**, *7* (2), 205–228.
- (27) Heerding, D. A.; Rhodes, N.; Leber, J. D.; Clark, T. J.; Keenan, R. M.; Lafrance, L. V.; Li, M.; Safonov, I. G.; Takata, D. T.; Venslavsky, J. W.; Yamashita, D. S.; Choudhry, A. E.; Copeland, R. A.; Lai, Z.; Schaber, M. D.; Tummino, P. J.; Strum, S. L.; Wood, E. R.; Duckett, D. R.; Eberwein, D.; Knick, V. B.; Lansing, T. J.; McConnell, R. T.; Zhang, S.; Minthorn, E. A.; Concha, N. O.; Warren, G. L.; Kumar, R. Identification of 4-(2-(4-amino-1,2,5-oxadiazol-3-yl)-1-ethyl-7-[[[(3S)-3-piperidinylmethyl]oxy]-1H-imidazo[4,5-c]pyridin-4-yl]-2-methyl-3-butyn-2-ol (GSK690693), a novel inhibitor of Akt kinase. *J. Med. Chem.* **2008**, *51* (18), 5663–5679.
- (28) Pal, S. K.; Reckamp, K.; Yu, H.; Figlin, R. A. Akt inhibitors in clinical development for the treatment of cancer. *Expert Opin. Invest. Drugs* **2010**, *19* (11), 1355–1366.
- (29) Blake, J. F.; Xu, R.; Bencsik, J. R.; Xiao, D.; Kallan, N. C.; Schlachter, S.; Mitchell, I. S.; Spencer, K. L.; Banka, A. L.; Wallace, E. M.; Gloor, S. L.; Martinson, M.; Woessner, R. D.; Vigers, G. P.; Brandhuber, B. J.; Liang, J.; Safina, B. S.; Li, J.; Zhang, B.; Chabot, C.; Do, S.; Lee, L.; Oeh, J.; Sampath, D.; Lee, B. B.; Lin, K.; Liederer, B. M.; Skelton, N. J. Discovery and preclinical pharmacology of a selective ATP-competitive Akt inhibitor (GDC-0068) for the treatment of human tumors. *J. Med. Chem.* **2012**, *55* (18), 8110–8127.
- (30) Kumar, R. IDiscovery of an oral Akt kinase inhibitor. *American Association for Cancer Research Annual Meeting*, Washington, DC, April 6–10, 2013.
- (31) Hauck, S. M.; Dietter, J.; Kramer, R. L.; Hofmaier, F.; Zipplies, J. K.; Amann, B.; Feuchtinger, A.; Deeg, C. A.; Ueffing, M. Deciphering membrane-associated molecular processes in target tissue of autoimmune uveitis by label-free quantitative mass spectrometry. *Mol. Cell. Proteomics* **2010**, *9* (10), 2292–2305.
- (32) Tai, A. W.; Salloum, S. The role of the phosphatidylinositol 4-kinase PI4KA in hepatitis C virus-induced host membrane rearrangement. *PLoS One* **2011**, *6* (10), No. e26300.
- (33) Levy, D. S.; Kahana, J. A.; Kumar, R. Akt inhibitor, GSK690693, induces growth inhibition and apoptosis in acute lymphoblastic leukemia cell lines. *Blood* **2009**, *113* (8), 1723–1729.
- (34) Rhodes, N.; Heerding, D. A.; Duckett, D. R.; Eberwein, D. J.; Knick, V. B.; Lansing, T. J.; McConnell, R. T.; Gilmer, T. M.; Zhang, S. Y.; Robell, K.; Kahana, J. A.; Geske, R. S.; Kleymenova, E. V.; Choudhry, A. E.; Lai, Z.; Leber, J. D.; Minthorn, E. A.; Strum, S. L.; Wood, E. R.; Huang, P. S.; Copeland, R. A.; Kumar, R. Characterization of an Akt kinase inhibitor with potent pharmacodynamic and antitumor activity. *Cancer Res.* **2008**, *68* (7), 2366–2374.
- (35) Altomare, D. A.; Zhang, L.; Deng, J.; Di Cristofano, A.; Klein-Szanto, A. J.; Kumar, R.; Testa, J. R. GSK690693 delays tumor onset and progression in genetically defined mouse models expressing activated Akt. *Clin. Cancer Res.* **2010**, *16* (2), 486–496.
- (36) Mallick, P.; Kuster, B. Proteomics: a pragmatic perspective. *Nat. Biotechnol.* **2010**, *28* (7), 695–709.
- (37) Lemeer, S.; Zörgel, C.; Ruprecht, B.; Kohl, K.; Kuster, B. Comparing immobilized kinase inhibitors and covalent ATP probes for proteomic profiling of kinase expression and drug selectivity. *J. Proteome Res.* **2013**, *12* (4), 1723–1731.
- (38) Carter, C. A.; Kane, C. J. Therapeutic potential of natural compounds that regulate the activity of protein kinase C. *Curr. Med. Chem.* **2004**, *11* (21), 2883–2902.
- (39) Hofmann, J. Protein kinase C isozymes as potential targets for anticancer therapy. *Curr. Cancer Drug Targets* **2004**, *4* (2), 125–146.
- (40) Teicher, B. A. Protein kinase C as a therapeutic target. *Clin. Cancer Res.* **2006**, *12* (18), 5336–5345.
- (41) Riento, K.; Ridley, A. J. Rocks: multifunctional kinases in cell behaviour. *Nat. Rev. Mol. Cell Biol.* **2003**, *4* (6), 446–456.
- (42) Dummmler, B.; Ohshiro, K.; Kumar, R.; Field, J. Pak protein kinases and their role in cancer. *Cancer Metastasis Rev.* **2009**, *28* (1–2), 51–63.
- (43) Heikkilä, T.; Wheatley, E.; Crighton, D.; Schroder, E.; Boakes, A.; Kaye, S. J.; Mezna, M.; Pang, L.; Rushbrooke, M.; Turnbull, A.; Olson, M. F. Co-crystal structures of inhibitors with MRCKbeta, a key regulator of tumor cell invasion. *PLoS One* **2011**, *6* (9), No. e24825.
- (44) Piazza, F.; Manni, S.; Semenzato, G. Novel players in multiple myeloma pathogenesis: role of protein kinases CK2 and GSK3. *Leuk Res* **2013**, *37* (2), 221–227.
- (45) Kim, H. M.; Kim, C. S.; Lee, J. H.; Jang, S. J.; Hwang, J. J.; Ro, S.; Choi, J. CG0009, a novel glycogen synthase kinase 3 inhibitor, induces cell death through cyclin D1 depletion in breast cancer cells. *PLoS One* **2013**, *8* (4), No. e60383.
- (46) Crouthamel, M. C.; Kahana, J. A.; Korenchuk, S.; Zhang, S. Y.; Sundaresan, G.; Eberwein, D. J.; Brown, K. K.; Kumar, R. Mechanism and management of Akt inhibitor-induced hyperglycemia. *Clin. Cancer Res.* **2009**, *15* (1), 217–225.
- (47) Assie, G. One single signaling pathway for so many different biological functions: lessons from the cyclic adenosine monophosphate/protein kinase A pathway-related diseases. *J. Clin. Endocrinol. Metab.* **2012**, *97* (12), 4355–4357.
- (48) Pearce, L. R.; Komander, D.; Alessi, D. R. The nuts and bolts of AGC protein kinases. *Nat. Rev. Mol. Cell Biol.* **2010**, *11* (1), 9–22.
- (49) Hofmann, F. The biology of cyclic GMP-dependent protein kinases. *J. Biol. Chem.* **2005**, *280* (1), 1–4.
- (50) Lincoln, T. M.; Dey, N.; Sellak, H. Invited review: cGMP-dependent protein kinase signaling mechanisms in smooth muscle: from the regulation of tone to gene expression. *J. Appl. Physiol.* **2001**, *91* (3), 1421–1430.
- (51) Lohmann, S. M.; Vaandrager, A. B.; Smolenski, A.; Walter, U.; De Jonge, H. R. Distinct and specific functions of cGMP-dependent protein kinases. *Trends Biochem. Sci.* **1997**, *22* (8), 307–312.
- (52) Orstavik, S.; Natarajan, V.; Tasken, K.; Jahnsen, T.; Sandberg, M. Characterization of the human gene encoding the type I alpha and type I beta cGMP-dependent protein kinase (PRKG1). *Genomics* **1997**, *42* (2), 311–318.
- (53) McAllister, F. E.; Niepel, M.; Haas, W.; Huttlin, E.; Sorger, P. K.; Gygi, S. P. Mass spectrometry based method to increase throughput for kinome analyses using ATP probes. *Anal. Chem.* **2013**, *85* (9), 4666–4674.
- (54) Schirle, M.; Bantscheff, M.; Kuster, B. Mass spectrometry-based proteomics in preclinical drug discovery. *Chem. Biol.* **2012**, *19* (1), 72–84.
- (55) Zhang, L.; Holmes, I. P.; Hochgrafe, F.; Walker, S. R.; Ali, N. A.; Humphrey, E. S.; Wu, J.; de Silva, M.; Kersten, W. J. A.; Connor, T.; Falk, H.; Allan, L.; Street, I. P.; Bentley, J. D.; Pilling, P. A.; Monahan, B. J.; Peat, T. S.; Daly, R. J. Characterization of the novel broad-spectrum kinase inhibitor CTx-0294885 as an affinity reagent for mass spectrometry-based kinome profiling. *J. Proteome Res.* **2013**.